



Spatio-Temporal Properties of Motion Detectors Matched to Low Image Velocities in Hovering Insects

D. C. O'CARROLL,*‡ S. B. LAUGHLIN,* N. J. BIDWELL,† R. A. HARRIS*

Received 29 October 1996; in revised form 9 June 1997

Our recent study [O'Carroll *et al.* (1996). *Nature* 382, 63–66] described a correlation between the spatio-temporal properties of motion detecting neurons in the optic lobes of flying insects and behaviour. We consider here theoretical properties of insect motion detectors at very low image velocities and measure spatial and temporal sensitivity of neurons in the lobula complex of two specialised hovering insects, the bee-fly *Bombylius* and the hummingbird hawkmoth, *Macroglossum*. The spatio-temporal optima of direction-selective neurons in these insects lie at lower velocities than those of other insects which we have studied, including large syrphid flies, which are also excellent hoverers. We argue that spatio-temporal optima reflect a compromise between the demands of diverse behaviour, which can involve prolonged periods of stationary, hovering flight followed by spectacular high speed pursuits of conspecifics. Males of the syrphid *Eristalis* which engage in such behaviour, have higher temporal frequency optima than females. High contrast sensitivity in these flies nevertheless results in reliable responses at very low image velocities. Neurons of *Bombylius* have two distinct velocity optima, suggesting that they sum inputs from two classes of motion correlator with different time constants. This also provides sensitivity to a large range of velocities.

Visual ecology Spatio-temporal Direction selectivity Motion detection

INTRODUCTION

As an animal moves through its world, the visual scene is transformed into a temporal sequence at the retina which depends on the velocity with which the animal moves as much as on the spatial structure of the scene. The best strategy for sampling and analysing this array of moving contrast features must therefore depend on the behaviour of the animal. With the constraints of small body (and hence eye size) and the limited optical capability of compound eyes (Kirschfeld, 1976; Land, 1981) and yet with enormous behavioural diversity, insects are an ideal group in which to examine the match between visual processing and the range of image velocities experienced by a particular eye. The velocity of optic flow experienced by a male fly while pursuing a conspecific at high speeds (Land & Collett, 1974) is several orders of magnitude greater than that associated with the near

stationary pose of a hovering hawkmoth sipping nectar on-the-wing (Farina, Varjú, & Zhou, 1994) or a solitary wasp approaching its nest entrance (Zeil, 1993).

Recent work on insect photoreceptors suggests that their response dynamics are closely matched to lifestyle. Fast, aerobic flies have photoreceptors that respond rapidly, allowing them to code the high temporal frequencies contained in rapidly moving images. Slower moving insects have photoreceptors with slower responses (Laughlin & Weckström, 1993; Weckström & Laughlin, 1995; Laughlin, 1996). Does matching of response dynamics to the demands of lifestyle also apply to visual processing at higher levels?

Behavioural and electrophysiological data for many animals, including primates, birds and insects, are consistent with a correlation-type mechanism for the detection of image motion (Hassenstein & Reichardt, 1956; Reichardt, 1957, 1961; Egelhaaf, Borst, & Reichardt, 1989; Borst & Egelhaaf, 1989; Buchner, 1984; Barlow & Levick, 1965; Wolf-Oberhollenzer & Kirschfeld, 1994; Wilson, 1985; van Santen & Sperling, 1985). In the blowfly, a small set of direction-selective, motion-sensitive cells with large receptive fields, described from the lobula plate (a specialised sub-region of the third optic ganglion), are a major component of the optomotor

*Department of Zoology, University of Cambridge, Downing Street Cambridge CB2 3EJ, U.K.

†Centre for Neuroscience, University of Sussex, Falmer BN1 9QG, U.K.

‡To whom all correspondence should be addressed [Tel: +44 1223 336657; Fax: +44 1223 336676; Email: dco1000@cus.cam.ac.uk].

pathway for flight stabilisation (Hausen, 1984; Hausen & Egelhaaf, 1989). Their physiology is consistent with input from an array of local motion detectors of the correlation type (Borst & Egelhaaf, 1989), as is the optomotor behaviour described from tethered flies (Pick & Buchner, 1979; Buchner, 1984). Previous work on such neurons in flies and butterflies shows that the time constant of neuronal responses adapts when cells are strongly stimulated with movement, particularly at high image contrast and velocity (Maddess & Laughlin, 1985; de Ruyter van Steveninck, Zaagman, & Mastebroek, 1986; Borst & Egelhaaf, 1987; Maddess, Dubois, & Ibbotson, 1991). This adaptation increases the sensitivity of the response to changes in image velocity (Maddess & Laughlin, 1985; Maddess *et al.*, 1991).

While motion adaptation may help to extend the range of velocities coded reliably by a lobula neuron during the aerial manoeuvres of many flying insects, less is known about how insect movement detectors cope with the demands of very low speed flight. Several insect orders include species which are excellent hoverers, able to maintain precise hovering flight for extended periods while feeding from flowers or awaiting the approach of conspecifics or prey. To see how hoverers maximise sensitivity to the low velocities which they experience during natural behaviour, we recently compared the spatial and temporal properties of motion-sensitive neurons of a diverse group of species drawn from three insect orders (O'Carroll, Bidwell, Laughlin, & Warrant, 1996). We showed that motion-sensitive neurons of the correlation type in the lobula complex of hoverflies and the nocturnal hawkmoth *Deilephila elpenor* are more sensitive to low image velocities than neurons of other species. This low velocity sensitivity results from differences in both spatial and temporal optima of neurons, as well as differences in absolute sensitivity.

We consider here how the basic properties of correlation-based motion detectors limit the spatio-temporal bandwidth of responses in a way which limits low velocity detection by compound eyes. We also extend our previous work by examining the spatio-temporal sensitivity of neurons in two specialist hovering species, the diurnal hawkmoth *Macroglossum stellatarum* and the bombyliid fly *Bombylius major*. Many hawkmoths (Sphingidae) hover with exquisite precision while feeding from flowers with an elongated proboscis. *Macroglossum* is both a superb hoverer and a strong and rapid flier, as evidenced by their migratory behaviour and rapid darts from flower to flower during foraging (Farina *et al.*, 1994; Farina, Kramer, & Varjú, 1995). Like sphingids, *Bombylius* is a nectar feeder and extends an elongated proboscis into flowers while supporting its body weight by hovering flight. Like some sphingids, *Bombylius* uses a tenuous grip on the flower, either with the front or rear pair of legs, to aid precise location of the proboscis while feeding. Up to the moment this grip is established and when manoeuvring in between flowers these flies hover precisely. Both males and females also hover in other situations. When laying eggs, *Bombylius*

females search suitable banks of soil for the entrances to the nests of solitary bees (*Halictus*, *Andrena*) on which it is a parasite. Having located a suitable hole, the fly hovers precisely in front of it and makes a series of extremely rapid forward darting motions, projecting an egg forward into the soil at the end of each and then returning to the hover. Males are "territorial hoverers" in a very similar manner to some syrphid flies. Thus, both sexes of these species face conflicting demands of detecting low image velocities while hovering and high image velocities when manoeuvring between flowers, pursuing conspecifics or laying eggs.

Finally, we describe the properties of the same neuron class in different sexes of the syrphid fly *Eristalis tenax*. Both males and females hover precisely when manoeuvring between nectar bearing flowers. Males, however, like males of many other flies (Land & Collett, 1974; Collett & Land, 1975) engage in vigorous territorial pursuits, at high speed, of other males, interspersed with extended periods of hovering within their territory (usually a shaft of sunlight filtering between overhead vegetation). Differences in the response tuning of the same neuron class in the two sexes provide important evidence that such tuning is associated with differences in behaviour.

METHODS

Recording

Animals were collected from the wild except for *Macroglossum stellatarum* which were kindly provided as pupae by Michael Pfaff and Almut Kelber from the Lehrstuhl für Biokybernetik, University of Tübingen. After emergence, *Macroglossum* adults were allowed to acclimatise to a natural light cycle for at least 3–4 days before experiments were performed. During this time they were observed to engage in normal flight and feeding behaviour.

Neurons were impaled intracellularly in the lobula complex of animals restrained by wax, using aluminium silicate glass micropipettes introduced through a small hole in the posterior head capsule. In some cases, neurons were identified anatomically after iontophoretic injection with 4% Lucifer Yellow CH (Sigma) using electrodes back-filled with 0.1 M LiCl. Lucifer filled electrodes gave very high tip resistance (300–1000 M Ω) and unstable, noisy recordings—unsuitable for the rigorous protocols which we performed. Most recordings were made, therefore, from neurons using electrodes filled with 1 M KCl (tip resistance approx. 100 M Ω) to obtain prolonged, stable intracellular recordings (up to 7 hr in some cases).

Experiments were performed under conditions as close as possible to those in which the insects would normally be active. Temperature is known to have a dramatic effect on the temporal properties of photoreceptors (e.g. Howard, Dubs, & Payne, 1984). Since this might affect temporal properties of motion detection we carried out all experiments at constant temperature. All species studied are active in bright sunlight and might be expected to

experience high head temperatures through absorption of radiant heat. We therefore selected the relatively high room temperature of 24°C.

Characterisation of neurons

Stimuli were presented on an XYZ display (Tektronix 608) with a mean luminance of approximately 60 cd/m² (equivalent to daylight/shade), at a frame rate of 200 Hz and driven by a Picasso Image Synthesiser under control of a Macintosh computer. The screen was positioned 7 cm in front of the animal, permitting production of patterns subtending approximately 70 deg. The rectangular image was masked with a circular aperture.

With the monitor initially positioned in front of the animal, general response properties (monitored on an oscilloscope and via an audio amplifier attached to a loudspeaker) were rapidly characterised qualitatively by stimulation with a drifting, diagonal grating of moderate contrast (approximately 0.35) and a spatial frequency of 0.1 cycles/deg. Neurons which responded selectively to alternation of motion direction with this orientation (a stimulus which drives either vertical or horizontal, direction-selective cells) were considered likely candidates for further study. Receptive field boundaries were located initially by moving a hand or finger at different locations around the animal, and the stimulus monitor was then centred on the receptive field. The degree of binocular input was then determined by blocking the view of each eye in turn with a small mask mounted on a manipulator or on a small piece of wood and held by hand. Neurons were only studied further if they had large receptive fields (responded beyond the boundaries of the stimulus screen).

During initial stimulation at a temporal frequency of 2 Hz, responses to sinusoidal gratings with a low enough contrast (typically 0.1) to avoid saturation of the response, were then plotted as the movement direction was varied in 16 steps from 0 to 360 deg over a period of a few seconds [see Fig. 2(b)]. Responses plotted as a function of direction allowed the approximate degree of direction selectivity and the preferred-null axis of the response to be determined rapidly, on-line. The optimum direction was then used for subsequent experiments. The neuron was then stimulated with a grating which increased linearly in temporal frequency from 1 to 40 Hz over a 10 sec period, again at low contrast. Response was then plotted as a function of temporal frequency, allowing a crude estimate of the temporal frequency tuning to be obtained. Providing the neuron fulfilled two criteria in response to these initial experiments—strong direction selectivity and distinct temporal frequency tuning, we carried out more detailed characterisation (see Results for further details of selection of neurons). Many neurons showed a graded response, either with or without a superimposed spiking response [e.g. Figure 2(a)]. In each case, the response of the cell was digitised using a GWI-625 data acquisition card in a Macintosh computer at a sample rate of 5 kHz, allowing

us to analyse either spiking or graded components of the response.

Spatio-temporal characterisation

Temporal frequency tuning was measured by adapting cells to a blank screen (mean luminance) for at least 5 sec prior to stimulation with a drifting, sinusoidal grating at one of 20 different temporal frequencies and at a spatial frequency of 0.1 cycles/deg. The effects of motion adaptation (Maddess & Laughlin, 1985; de Ruyter van Steveninck *et al.*, 1986; Borst & Egelhaaf, 1987; Maddess *et al.*, 1991) on the shape of these curves was minimised by using a short stimulus duration (500 msec) and a low contrast of approximately 0.1 (O'Carroll *et al.*, 1996). As we reported previously (O'Carroll *et al.*, 1996), under these conditions there is little evidence of large response transients and responses were observed to come to steady state within the first 200–300 msec of stimulation. The data obtained thus represent the temporal frequency response tuning in an “unadapted” state such as that which might be experienced by a stationary animal which commences moving, or during hovering.

We developed a rapid “ramp” method to determine contrast thresholds at many combinations of spatial and temporal frequency. The cell was first adapted to a blank screen of mean luminance for 10 sec. The contrast of a drifting grating was then increased linearly for 10 sec, over the contrast range 0–1.0. The shape of the response measured during a contrast ramp at near optimal spatial and temporal frequency approximated the relationship between response and contrast obtained by conventional means with drifting gratings presented at several different constant contrast levels (see Fig. 4). Small lateral shifts are introduced by the response latency, but latency measured in contrast “step” experiments (as above) was in the order of 15–30 msec for the neurons described here, which was smaller than the bin size (50 msec) used to smooth the ramp response (see Fig. 4). After subtracting the mean response during the pre-stimulus period, the contrast required for the ramp response to exceed a noise-based criterion was taken as the threshold. The criterion used was the standard deviation of the raw graded response in a control experiment (where the neuron viewed the blank screen for 12 sec). This criterion level is thus the level of “spontaneous” noise of the cell at the mean luminance of the screen (typically 10–20% of the maximum response level) and is probably a conservative measure of “detectability” for a particular pattern. Traditional techniques for contrast sensitivity determination (e.g. “Staircase” protocols) which might lead to greater estimates of sensitivity than ours, are very laborious and with intracellular recordings, technically demanding. This method is sufficiently rapid to allow us to determine contrast sensitivity in 1–2 hr intracellular recordings from up to 200 combinations of spatial and temporal frequency.

Modelling

A simple model of correlation EMDs [see Fig. 1(a)]

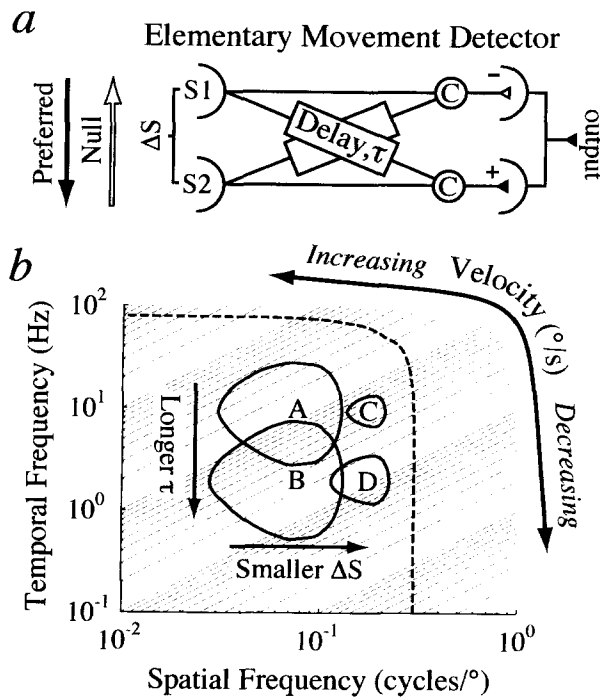


FIGURE 1. (a) A summary of the correlation model used to account for the direction-selective responses of neurons to image motion. The preferred direction for this elementary motion detector (EMD) is indicated by the arrows. (b) The spatiotemporal response of a computer simulation of four EMDs (A, B, C and D) organised as in (a), but utilising different combinations of delay time constant, τ and spatial separation of the inputs, Δs . The different time constants selected yield temporal frequency maxima at approximately 10 and 2 Hz (Borst & Bahde, 1986). Diagonal lines of equal velocity are shown faintly in the background. The contour level shown for each EMD represents the half-maximal response level of EMD B. We assumed spatial and temporal pre-filtering of the inputs S1 and S2 typical of photoreceptors of diurnal flies (see Methods). The dashed line encompasses the region at which the amplitude gain of the pre-filters is greater than 50%.

was implemented using Matlab software (version 5.0) running on a PC. We used a sinusoidal waveform as an input sequence to the two sampling stations S1 and S2, with a nominal sample rate of 500 Hz and a period determined by the temporal frequency of the test condition. A phase difference was introduced to the input sequence at S2, corresponding to the spatial separation of the inputs [Δs in Fig. 1(a)] and the desired spatial frequency of the stimulus. The inputs were then pre-filtered by spatial and temporal low-pass filters based on properties of typical fly photoreceptors. The temporal filter was a log-normal function (Payne & Howard, 1981) with a time to peak of 10 msec and a width parameter, σ , of 0.23. This results in a temporal transfer function typical of diurnal flies (Howard *et al.*, 1984; Laughlin & Weckström, 1993). The spatial filter was a gaussian acceptance function with a half-width of 1.48 deg, slightly narrower than for typical fly photoreceptors (Hardie, 1985).

The EMD delay was implemented by convolving the pre-filtered signal in the delayed channel with the impulse response of a first-order exponential filter (as

used by Clifford, Ibbotson, & Langley, 1997). The impulse response $h(t)$ of this filter is given by

$$h(t) = k.e^{-\frac{t}{\tau}}$$

where τ is the time constant and k was selected to give a gain of unity, as defined by the integral of the impulse response.

The non-linear correlation interaction [C in Fig. 1(a)] was implemented by multiplication of the delayed and undelayed sequences. The output sequence from a similar operation for a "mirror sub-unit" [see Fig. 1(a)] was then subtracted to give the final EMD output. The steady state output level was averaged over one complete cycle of the input sequence. We ran this simulation at 260 combinations of spatial frequency (between 0.01 and 1 cycles/deg) and temporal frequency (between 0.1 and 100 Hz). We repeated this for four different EMD types using two different values of Δs (3 and 1 deg) and two different values of τ (15.92 and 79.58 msec). After cubic interpolation onto a larger matrix (100 spatial frequencies by 150 temporal frequencies), a plot with a contour representing the 50% maximal response level for EMD B [Fig. 1(b), where Δs is 3 deg and τ is 79.58 msec], was then constructed for each of the four spatio-temporal responses. A further simulation, aimed at approximating the spatio-temporal data we obtained for *Bombylius*, used a Δs of 1.43 deg and τ of 113 msec. The response of this simulation was then scaled to the measured maximum sensitivity of a *Bombylius* neuron, so that contour lines equivalent to those in the measured spatio-temporal sensitivity plot could be plotted. In both plots (Fig. 5), contours were plotted at contours representing sensitivity of 2, 5, 10 and 20 (threshold contrasts of 50, 20, 10 and 5%, respectively) as for previously published data for other insects and humans (O'Carroll *et al.*, 1996; Kelly, 1979).

RESULTS

Motion correlation and velocity

A simplified version of the correlation model for motion detection originally introduced by Hassenstein & Reichardt (1956) is illustrated in Fig. 1(a). Two inputs, S1 and S2 sample adjacent points in an image and are compared (C) by a non-linear interaction after a delay (τ) in one sample. The output of a "mirror" sub-unit, with opposite polarity but comparing the same two points, is then subtracted. This whole operation is generally considered to represent an "elementary movement detector" (EMD). Although the underlying mechanism of the delay has not been established, "classic" versions, such as the Hassenstein & Reichardt (1956) model, implement it as a low-pass filter with a time constant, τ . Specific implementations of the model also include varying degrees of spatial and temporal low-pass or high-pass filtering of the inputs [S1 and S2 in Fig. 1(a)] or outputs of the EMD in order to account for the effects of optical and physiological properties of typical visual systems (e.g. Hassenstein & Reichardt, 1956; Buchner,

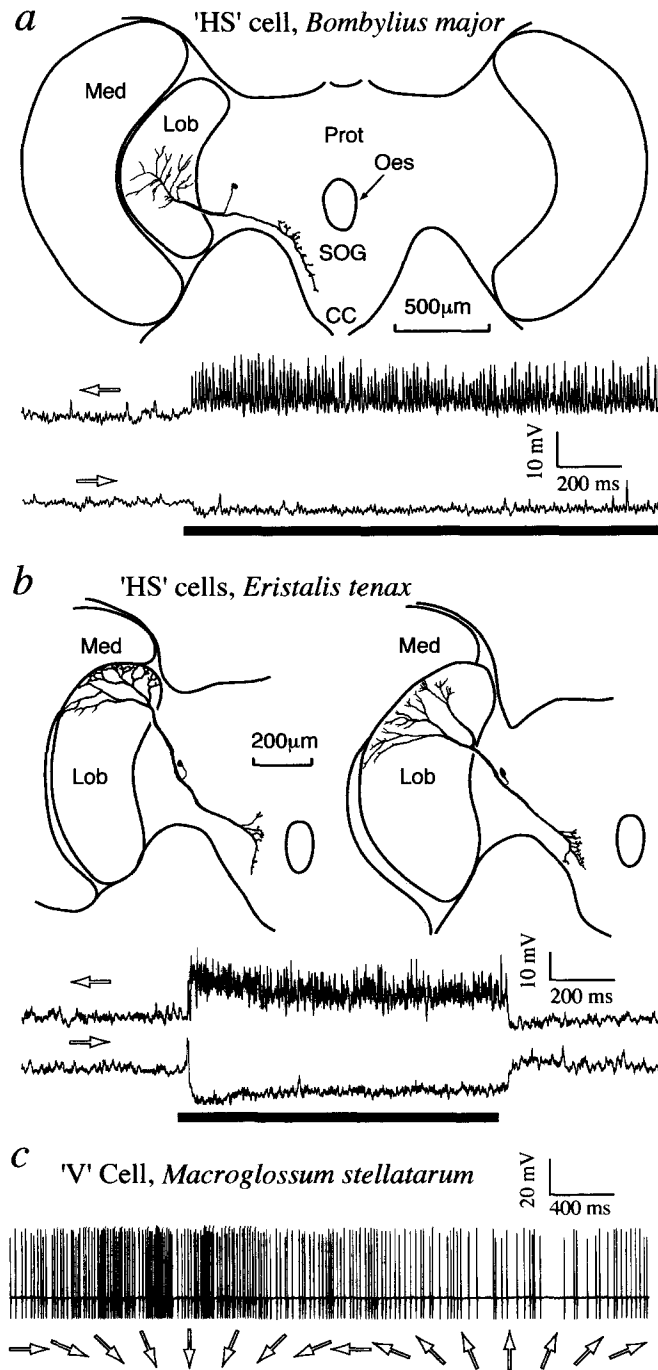


FIGURE 2. (a) An anatomical reconstruction and responses of a direction-opponent neuron in the lobula plate of *Bombylius*, with large graded responses. Responses to motion (in the direction indicated by the arrows) for the period indicated by the dark bar are shown for both preferred (corresponding to “progressive” or “front-to-back” motion) and null (“regressive”) directions. Both anatomy and response characteristics are similar to HS neurons previously described from the lobula plate of other flies (Hausen, 1984). Abbreviations: Med, medulla; Lob, lobula complex; Prot, protocerebrum; Oes, oesophageal foramen; SOG, sub-oesophageal ganglion; CC, cervical connective. (b) Shows data for two similar neurons in *Eristalis*. The physiological responses are for the more equatorial unit (right-hand). (c) Shows responses of a “V” cell—a vertical (downward), direction-selective neuron in *Macroglossum*. The neuron was stimulated by a constantly drifting pattern, which was “stepped” through 16 different stimulus directions (at the times indicated by the direction arrows). By keeping contrast low (0.1 in this case) saturation effects are minimised, allowing direction selectivity to be rapidly characterised.

1984; van Santen & Sperling, 1985). The essential properties of a non-linear interaction (usually presumed to resemble multiplication) between delayed and undelayed inputs which view adjacent points in space are,

however, common to all of these implementations (Kirschfeld, 1972; Buchner, 1984; Egelhaaf *et al.*, 1989).

What are the consequences of these basic properties for the detection of low velocities of motion? A periodic

grating of spatial frequency f_s moving at velocity V , produces a temporal frequency, f_t , (the frequency with which each stripe passes a fixed point in space) according to the following:

$$f_t = V f_s \quad (1)$$

A prediction of either minimal or elaborated versions of the correlation model when considering responses to periodic gratings, is that the delay time constant, τ , tunes an EMD (and thus any neuron or behaviour driven by an array of EMDs) to an optimum temporal frequency of the grating, rather than to its velocity (Buchner, 1984; Egelhaaf *et al.*, 1989). The output of a correlator also depends, in a critical way, on the spatial separation of the inputs, Δs [Fig. 1(a)]. Output is maximal when the spatial phase difference between the inputs is 90 deg, i.e. for a grating with a spatial frequency $1/4\Delta s$ (Buchner, 1984). The spatial separation also sets an upper limit on the spatial frequencies which can be usefully analysed, since any spatial frequencies above $1/2\Delta s$ will produce spatial "aliasing" (Buchner, 1984).

Since the time constant, τ , of the correlator delay mechanism tunes an EMD to temporal frequency and the spatial separation Δs of the inputs tunes it to spatial frequency, it follows from Eq. (1) that correlation-type motion detectors are tuned in the spatio-temporal domain to an "optimum" image velocity, V_{opt} . Hence:

$$V_{\text{opt}} \propto \Delta s / \tau \quad (2)$$

Is detection of low image velocities a problem for insect motion correlators? Considering Eq. (2), it can be seen that sensitivity to low velocities could be achieved in several ways. Correlators could use a large delay time constant, τ . As an alternative, correlators with a smaller spatial separation of the inputs, Δs , would also have a low optimum velocity.

Outputs of model EMDs

We implemented a simple computer model of EMDs organised as in Fig. 1(a) to investigate the effects of varying the delay time constant, τ or the spatial separation, Δs , of otherwise identical inputs. EMD A is tuned to the highest velocities [Fig. 1(b)] by using a short delay time constant, τ (15.92 msec) and a large spatial separation of the inputs, Δs (3 deg). EMDs B and C are tuned to a lower velocity than A, through a longer delay time constant, τ (79.58 msec) in B and a smaller spatial separation of the inputs, Δs (1 deg) in C. EMD D is tuned to the lowest velocities (approximately 1/10 that of A) through both a small spatial separation of the inputs, Δs (1 deg) and a longer delay time constant, τ (79.58 msec) than type "A".

Applying a criterion of constant response, a narrower range of velocities are encompassed by EMDs C or D than EMD A [Fig. 1(b)]. This is because the spatio-temporal optimum is shifted towards spatial frequencies where the low pass filtering effects of the optics become significant. This decrease in signal power at high spatial frequencies is a particular problem for motion detection at low velocities by compound eyes. Optical blur

resulting from diffraction at each facet places a practical constraint on $\Delta\phi$, the spatial separation of photoreceptors (Kirschfeld, 1976) and the spatial separation of the correlator inputs, Δs , cannot be smaller than $\Delta\phi$. Thus, Δs is severely constrained by eye size, since smaller separations require more facets and each facet must be larger to counter the effects of diffraction.

Comparison of EMDs A and C with the longer time constant EMDs (B and D) shows that the bandwidth is also somewhat reduced in EMDs with short delay time constants, τ , as the spatio-temporal optimum approaches temporal frequencies, where the low-pass filtering introduced by the temporal properties of photoreceptors becomes significant. Note that this effect is much weaker than the effect of spatial filtering, despite our selection of a time constant, τ , for EMDs A and C of 15.92 msec, which yields a temporal frequency optimum of 10 Hz (Borst & Bahde, 1986). This is relatively high compared with several species of diurnal flies (where the temporal frequency optimum is 6–8 Hz; O'Carroll *et al.*, 1996).

Because of the characteristic spatial and temporal filtering produced by τ and Δs , motion correlation can thus be regarded as a spatio-temporal band-pass filtering operation. The effects of noise introduced in photoreceptor responses and by subsequent levels of processing will degrade the reliability of EMD outputs. The resultant degradation of the useful sensitivity of the detector will become more severe at image velocities further from the optimum. It is thus likely that in the evolution of visual systems for "real-world" tasks, high sensitivity (and thus reliability) is invested at spatial and temporal frequencies which correspond to velocities which are most likely to be experienced.

Selection of neurons

Do neurons of "specialist" hovering insects show properties consistent with hypothetical EMDs for detection of low velocities? We address this question using single unit intracellular recordings from the lobula plate of "specialist" hovering moths and flies. With this approach we cannot be certain that the neurons we record are directly involved in hovering. However, we screened more than 30 different types encountered in each species and selected those which, on the basis of their receptive field properties, are most likely to be involved in flight stabilisation. The selection was made as follows.

Cells were initially classified on the basis of a rapid determination of their directional selectivity, receptive field sizes and response to a range of temporal frequencies (Methods). We found several classes of neuron in each species with a variety of receptive field sizes from approximately 40 deg across to whole-field ipsilateral, contralateral or binocular units. Neurons with different preferred directions, both horizontal and vertical, were encountered in each species (Fig. 2). It is important to note that all cells that were strongly direction-selective responded to a similar range of temporal frequencies.

We then selected direction-selective neurons with

large ipsilateral/frontal receptive fields for a more detailed analysis because, by analogy with the neurons in the lobula plate of the blowfly *Calliphora*, these are most likely to be involved in the stabilisation of flight. In *Calliphora*, these criteria would limit inclusion to cells designated V, H, VS and HS, which are directly implicated in generation of compensatory optomotor responses to wide-field motion (Hausen, 1984; Hausen & Egelhaaf, 1989). We cannot be confident of homology with these blowfly neurons, because the neuroanatomy and physiology of the species we have selected have not yet been studied in sufficient detail. Nevertheless, in some cases (Fig. 2) we stained neurons by Lucifer yellow injection and their anatomy was always reminiscent of typical examples of lobula plate "tangential" neurons in *Calliphora*, with fan-like arborizations in the lobula plate and an axon which terminates either in the ipsilateral or contralateral deutocerebrum or which crosses to the contralateral lobula plate.

Figure 2(a) shows data for an anatomically labelled neuron from the bombyliid fly *Bombylius major* with very similar physiology and anatomy to the identified HSE neuron described in the lobula plate of *Calliphora* (Hausen, 1984). Like HSE, this unit had an equatorial receptive field and a strong preference for front to back (progressive) motion, with small "spikelets" superimposed on a graded response, and with equal degrees of depolarisation and hyperpolarisation upon stimulation with patterns moving in the preferred and null directions [Fig. 2(a)]. The positions of the cell body and the heavily beaded output dendrites in the lateral deutocerebrum (close to the inputs to descending interneurons in the suboesophageal ganglion) are very similar to those of HS cells in *Calliphora* (Hausen, 1984; Hausen & Egelhaaf, 1989). The position of arborization in the lobula plate is also reminiscent of that of HSE, although the axon and (presumed) input dendrites in the lobula plate are much narrower and there is a more compact and restricted dendritic tree.

We were able to record from neurons that were physiologically indistinguishable from that illustrated in Fig. 2(a), in several individuals of *Bombylius*. Most data we describe here for this species are from such neurons. We also recorded from similar, "HS-like" neurons in the syrphid flies *Volucella pelluscens* and *Eristalis tenax* [NB: the data obtained for the cell in Fig. 3(c) of O'Carroll *et al.*, 1996 is from also from an "HS" type neuron]. Figure 2(b) shows reconstructions of 2 Lucifer labelled HS neurons in *Eristalis*. One neuron had a strictly dorsal receptive field, corresponding approximately to that described for the blowfly HSN cell (Hausen, 1984). The second neuron has a much more equatorial receptive field, both anatomically and physiologically and was more typical of those included in this study. As in the *Bombylius* HS-like neurons, the graded physiological response of this cell class is both characteristic and indistinguishable from blowfly HS cells [Fig. 2(b)]. The numbers and anatomy of lobula plate neurons is known to vary between fly species, in a

manner which may be correlated with differences in behaviour (Buschbeck & Strausfeld, 1996). Further unidentified neurons with HS-like physiology and with equatorial/ventral and ventral receptive fields were also encountered in *Eristalis* and it thus seems possible that there may be four HS cells in this species, compared with three in the blowfly.

We were not able to locate "HS-like" neurons in the sphingid moth *Macroglossum*, but nevertheless encountered spiking neurons which responded maximally to either downward [Fig. 2(c)] or front-to-back (progressive) motion, and with very similar receptive field location. We decided to use this latter class of horizontal, progressive motion-sensitive neurons, with frontal/equatorial receptive fields, as the basis for comparisons with the HS-like neurons of Diptera and data published for neurons in other species (O'Carroll *et al.*, 1996). While we recorded from many additional neurons which might be involved in analysis of other components of optic flow, we are thus restricting our description here to neurons which, like the HS cells of other flies, are very likely to be involved in analysis of rotational or horizontal translation components of optic flow.

Temporal frequency tuning

Figure 3 shows the temporal frequency response to gratings of moderate contrast (0.1) in *Bombylius* and *Macroglossum*. These data were obtained at a spatial frequency of 0.1 cycles/deg, close to the optimum for the neurons, but qualitatively similar curves (though with weaker responses) were derived for each neuron at both higher and lower spatial frequencies. Data for both species show a profound reduction in response above 10 Hz. Fast flying, diurnal insects have "fast" photoreceptors, with excellent modulation at frequencies in excess of 50 Hz (Laughlin & Weckström, 1993; Weckström & Laughlin, 1995), so it is very unlikely that this attenuation can be attributed to low-pass filtering by photoreceptors. In *Macroglossum* at least, the shape of the response curve agrees with the output of a motion detector operating by correlation in showing a broad optimum, centred close to 2 Hz. This agrees closely with similar data for neurons in other sphingids (O'Carroll *et al.*, 1996). It is also close to the optimum modulation frequency for compensatory responses to drifting, striped patterns, determined by behavioural analysis of this species (Farina *et al.*, 1995), which strengthens our argument that such neurons are likely to play a role in stabilising hovering. In *Bombylius*, responses at low temporal frequencies are similar to those in *Macroglossum* and other sphingids, but the "optimum" region is even broader, with two peaks apparent in the data, one close to 1 Hz and a second at 8 Hz. *Bombylius* "HS" neurons continue to respond strongly to temporal frequencies beyond 40 Hz, even at the low contrast (0.1) used.

Spatio-temporal sensitivity in *Bombylius*

To be sure that tuning to low temporal frequencies

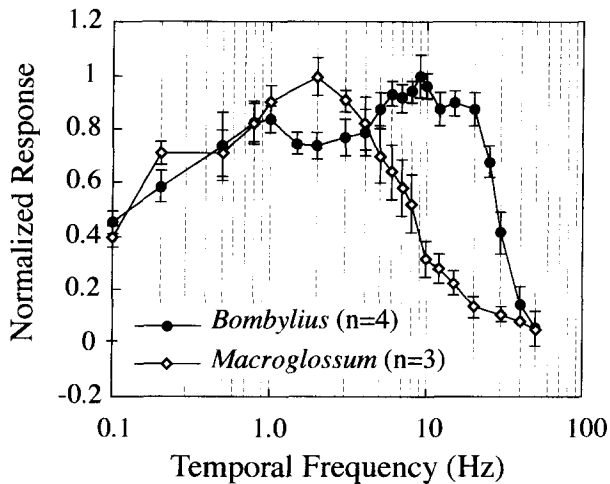


FIGURE 3. Temporal frequency tuning curves determined using sinusoidal gratings of moderate (non-saturating) contrast drifted in the preferred direction of neurons from *Macroglossum* and *Bombylius*. All data are for neurons selective for “progressive”, horizontal motion [e.g. Figure 2(a)], with frontal, equatorial receptive fields. Data for *Bombylius* are for “HS”-like neurons as in Fig. 2(a). Data are the mean responses (\pm SE) from several recordings in different individuals.

confers useful sensitivity to low velocities, we also considered the spatial tuning and the contrast sensitivity of neurons. Contrast sensitivity reflects the signal to noise ratio of the motion detection pathway and thus provides a measure of the useful limits of performance. The “contrast ramp” method that we developed is sufficiently rapid to permit determination of contrast sensitivity at many combinations of spatial and temporal frequency during intracellular recordings of 1–2 hr duration. The response of neurons during the contrast ramp approximates that obtained by a more laborious procedure of presentation of the stimulus at different contrasts after adaptation to a blank screen of mean luminance (Fig. 4). Some cells, like the “HS” cell in *Volucella*, illustrated in Fig. 4, are sufficiently sensitive at low contrasts that the response saturates early in the ramp. Subsequent motion adaptation then depresses the ramp response at higher contrasts, relative to that obtained by the other method. Close to the response threshold (indicated by the dashed line in Fig. 4) these two curves are very similar. Indeed, using both methods, this cell was sensitive enough to track small deviations in effective contrast at each DAC control voltage (indicated by the arrows) due to non-linearities in the contrast control for the display monitor (these were allowed for before contrast sensitivity was solved).

Spatio-temporal sensitivity measurements made using this ramp method show that the large differences observed in temporal frequency tuning of supra-threshold responses do indeed shift the range of velocities to which neurons are sensitive (O'Carroll *et al.*, 1996). A complete spatio-temporal threshold surface for a neuron in *Bombylius* is shown in Fig. 5(a). It shows similar sensitivity at very low velocities to that we described for an HS-like neuron in the large syrphid fly *Volucella*

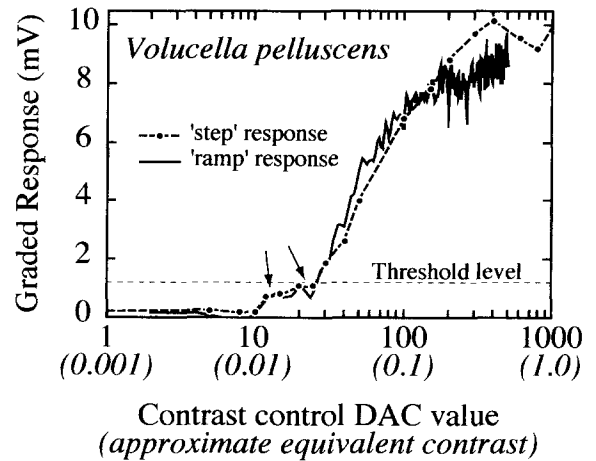


FIGURE 4. The graded response of an HS-like neuron in the syrphid fly *Volucella pelluscens* plotted as a function of the digital to analogue converter (DAC) control value fed into the voltage-sensitive contrast input on the stimulus generator (Picasso). The solid line shows the response during a single contrast ramp (see Methods) of a grating drifting at 2 Hz temporal frequency and at a spatial frequency of 0.2 cycles/deg. The response was smoothed by binning 50 msec segments. The DAC control value was varied during the ramp from 0 to 1000, resulting in an approximately linear ramp over time) of grating contrast from 0 to nearly 1.0 (as indicated in the axis labels in parentheses). Dotted lines with solid symbols represent the graded response measured after adaptation to a blank screen for 5 sec followed by a 200 msec presentation of gratings with the same spatial and temporal frequency, at 20 different contrasts (presented in random order). The arrows indicate the response near DAC values of 10–20, where non-linearities in the Z-gain amplifier and phosphor of the display produce a non-linearity in the relationship between the nominal control value and the actual stimulus contrast.

(O'Carroll *et al.*, 1996). Interestingly, this is despite the minimum detectable contrast being just below 0.05, compared with below 0.01 in *Volucella*, and a spatial optimum at approximately 0.1 cycles/deg compared with the higher optimum of 0.15 cycles/deg in *Volucella*.

How does *Bombylius* achieve such high sensitivity to very low image velocities despite a lower overall sensitivity and a lower optimum spatial frequency than *Volucella*? A possible explanation is the combination of more than one temporal class of EMD to the response of the wide-field unit, as suggested by two distinct “peaks” visible in the spatio-temporal sensitivity surface, at similar spatial frequency but at different temporal frequencies (1 and 5 Hz). Two peaks are also visible in the responses illustrated in Fig. 3 and were observed in many other cells (not shown) from this species. The higher of the two temporal frequency peaks in Fig. 5(a) corresponds to a velocity optimum of approximately 40 deg/sec—similar to velocity optima of neurons for two other hoverers, the nocturnal sphingid moth *Deilephila* and the large syrphid fly *Volucella* (O'Carroll *et al.*, 1996). The lower sensitivity peak, at just 15 deg/sec is lower than in any species we have previously studied (O'Carroll *et al.*, 1996). Tuned as it is to low velocities, this neuron shows little sensitivity above 1000 deg/sec.

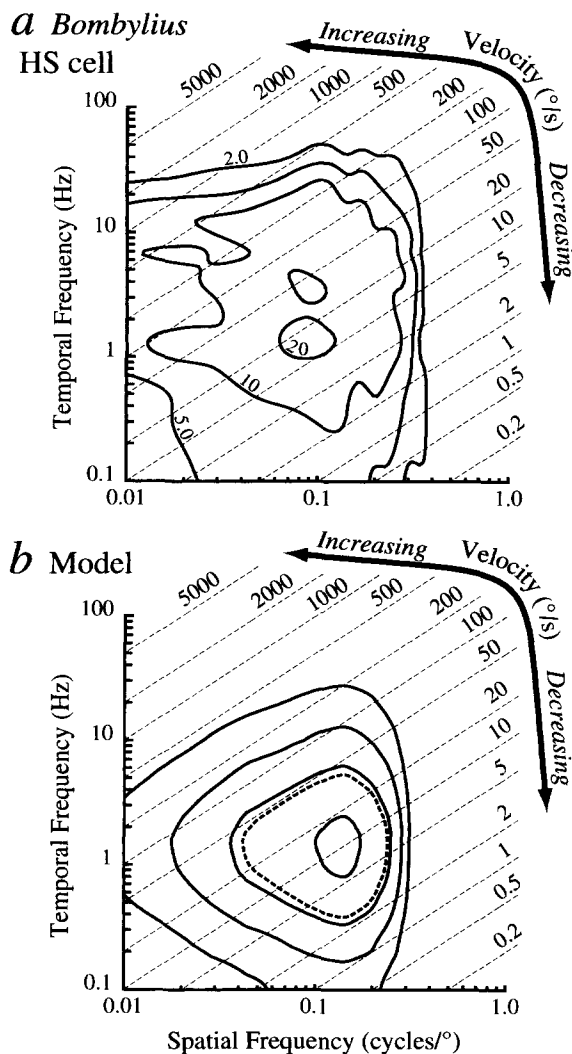


FIGURE 5. (a) A spatio-temporal contrast sensitivity plot for an HS-like neuron in *Bombylius*. Contour levels are $1/\text{threshold contrast}$ (the stimulus contrast required to evoke a significant response) determined from contrast ramps at 200 combinations of spatial and temporal frequency. Note the “dual peaked” temporal frequency tuning which extends sensitivity across a large velocity range. Contour lines were fitted by quadratic spline interpolation of the sensitivity data, using Matlab software (version 4.2 for Macintosh) and are $1/\text{threshold contrast}$. (b) Shows a model fit to the data in (a). For details, see Methods. Contour levels are the same as in (a) after normalizing the model output to the maximum of the cells’ response [in (a)]. The dashed line shows the 50% response level, which is close to the contour representing a contrast sensitivity of 10.

We used the computer model described earlier to see if the observed spatio-temporal surface could be accounted for by a single EMD class. Figure 5(b) shows the spatio-temporal output of a model EMD with a 113 msec delay time constant and a spatial separation of 1.43 deg. These values were selected to yield a temporal frequency optimum equivalent to that of the lower peak, and a spatial frequency cut-off of 0.35 cycles/deg (similar to that observed). The resulting surface, normalized with respect to the maximum in the measured data, provides an excellent fit to the low temporal frequency/high spatial frequency characteristics of the observed data. However,

while the half-maximal output level of the model EMD (the dashed line) does not extend beyond 50 deg/sec, a similar sensitivity level (contrast sensitivity = 10) in the neuron extends well beyond 200 deg/sec. The model optimum response is at a slightly higher spatial frequency than is observed in the neuron, suggesting that there is some contribution from a second EMD class with a larger spatial baseline, as observed previously in flies (Buchner, 1984). This is still not sufficient to account for the broadness at high temporal frequencies, however, since in the temporal frequency domain, the 50% response level of the model is at just 5 Hz, compared with over 20 Hz in the neuron.

The broadness in tuning could possibly be accounted for if the EMDs utilised a very different delay filter to the simple first-order filter we have used in our model. A further observation, however, is difficult to account for with a single temporal EMD class, even with a delay filter with a very “broad” impulse response. While the contrast sensitivity of the neuron in Fig. 5 is similar at the two peaks, Fig. 3 suggests that the upper peak is more prominent in responses at moderate contrasts. This is reinforced by Fig. 6, which shows the temporal tuning of a spiking neuron with a similar receptive field and direction selectivity to the HS-like cells. Figure 6(a) is the mean response at a relatively high contrast (0.4) and Fig. 6(b) shows the contrast sensitivity for the same neuron. The lower peak is very prominent in the sensitivity plot at an even lower temporal frequency than in Fig. 5, but also gives rise to a similar, broadly tuned response at high contrasts.

Spatio-temporal sensitivity in Macroglossum

We have not yet obtained intracellular recordings from neurons in *Macroglossum* of sufficient duration to derive an entire spatio-temporal threshold surface. However, Fig. 7 shows the spatial contrast sensitivity pooled from four horizontal, front-back (progressive) motion-sensitive cells in *Macroglossum*, determined at the near-optimal temporal frequency of 2 Hz. The spatial optimum in this species is at 0.1 cycles/deg. These cells had rather small receptive fields (barely responding beyond the boundaries of the frontally placed screen) compared with the HS cells we find in flies. Another cell we recorded from, however, with a larger receptive field, responded reliably to grating contrasts close to 2%, indicating greater overall contrast sensitivity (>50) than in any of the other species we have recorded from except *Volucella* (O’Carroll *et al.*, 1996).

In *Macroglossum*, the spatial optimum of 0.1 cycles/deg (Fig. 7) and temporal optimum of 2 Hz (Fig. 3) results in a velocity optimum close to 20 deg/sec, nearly as low as the lower of the two peaks in *Bombylius*. Two of the neurons included in the data in Fig. 7 still responded to contrasts below 0.5 at a grating temporal frequency of 0.2 Hz and a spatial frequency of 0.3 cycles/deg. Considering that the temporal tuning data for this species (Fig. 3) show strong sensitivity even at 0.1 Hz, it is likely that useful sensitivity extends below 0.5 deg/sec.

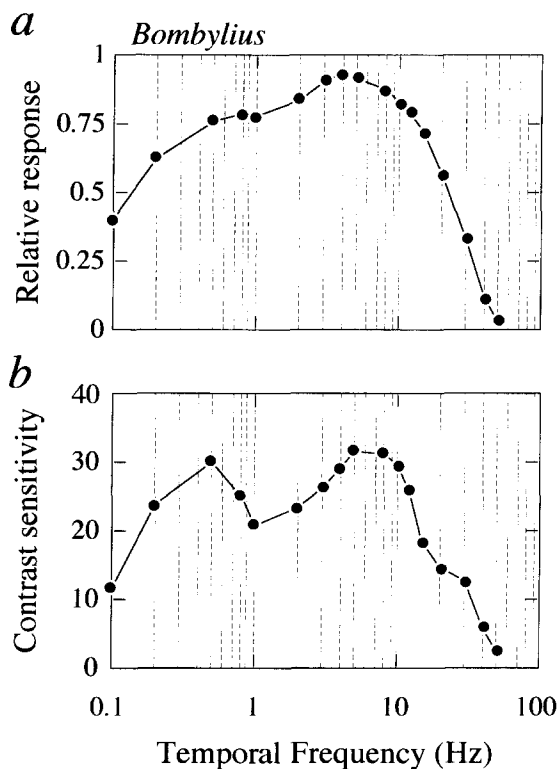


FIGURE 6. Temporal responses of an “H” type (horizontal, “progressive” motion selective) spiking neuron in *Bombylius*. (a) Shows the response at moderate contrast (0.4) to a grating with a spatial frequency of 0.1 cycles/deg, drifted in the preferred direction. (b) Shows the contrast sensitivity ($1/\text{threshold contrast}$) derived from contrast ramps. The sensitivity optimum evident at low temporal frequency in (b) “saturates” in the higher contrast response illustrated in (a), which although broadly tuned, is dominated by the sensitivity peak centred near 6 Hz.

Sex differences

The relationship between behaviour and velocity tuning is further strengthened by comparisons of the properties of the same class of neuron in different sexes. Figure 8 shows temporal tuning of HS-type neurons from the lobula plate of males and females of the syrphid *Eristalis tenax*, measured while stimulating the neurons equatorially (i.e. with the stimulus monitor close to the “horizon” of the body axis). Compared with females, the temporal frequency tuning of HS-type neurons from the lobula plate of males of *Eristalis* are shifted to higher frequencies than their female counterparts (Fig. 8). Although dimorphism in local inter-receptor angles associated with the “love-spot” of the male eye in large syrphids may result in a slightly higher spatial frequency optimum in the dorsal part of the receptive fields, equatorial acuity is similar in the two sexes (Olsson, Warrant and O’Carroll, unpublished data). In *Eristalis*, the overall eye size of male and female *Eristalis* are also very similar (average diameter 3.0 mm in males and 2.8 mm in females). These differences may thus result in tuning to higher velocities in males than in females, consistent with the demands of high speed flight experienced by males during territorial encounters.

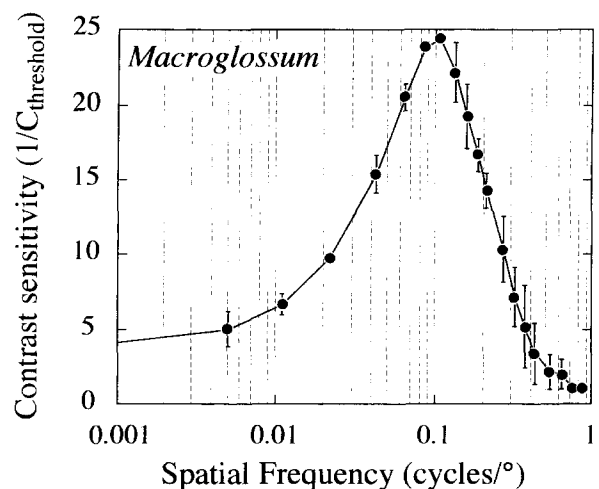


FIGURE 7. Spatial contrast sensitivity of horizontal, progressive motion-selective neurons in the hummingbird hawkmoth *Macroglossum*, determined from contrast ramps at the optimum temporal frequency of 2 Hz. Data are the mean sensitivity, $1/\text{threshold contrast}$ (\pm SE) from four cells in different individuals.

DISCUSSION

Hovering and analysis of low velocities

“Hovering” can be defined as a condition where the velocity and accelerations of the airborne animal are minimal and maintained that way for an extended period (Ellington, 1984). No control system can be expected to be noise-free and the world in which an insect flies is inherently irregular (e.g. due to the effects of wind). Therefore, in addition to the aerodynamic demands of the task, hovering requires a control system to detect and compensate for small perturbations of the body generated about the same axes of yaw, pitch and roll as are important for controlling “progressive” flight. Although other visual mechanisms, such as positional stabilisation of small targets (Land, 1992) and other sensory systems (Nalbach & Hengstenberg, 1994) play an important role, analysis of optic flow across the retinas of the compound eyes is one obvious cue available to stabilise position while hovering (Farina *et al.*, 1995). As hovering approaches “perfection”, the image velocities induced by ego-motion will approach zero, irrespective of the structure of the surrounding world (such as the distance to nearby objects).

If the compensatory optomotor response to rotational motion is driven by inputs from motion detectors such as those which we describe, it is very likely that the ability of an insect to maintain stable hovering is limited, in part, by their sensitivity to low image velocities.

Are HS-like cells used for stabilisation of hovering?

Although no data addressing this question directly are available for hovering flies such as syrphids or *Bombylius*, extensive work on the compensatory torque responses of other flies as behaviourally diverse as *Drosophila* and the blowfly *Calliphora* suggests that the response to rotational components of optic flow is also

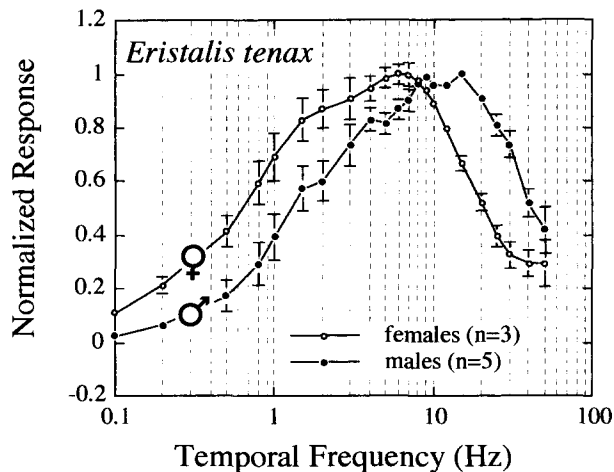


FIGURE 8. Sexual dimorphism in temporal frequency tuning of neurons from the hoverfly *Eristalis tenax*. All data are “equatorial” responses of HS-like neurons to sinusoidal gratings of moderate contrast, drifted in the preferred direction. Neurons from males are clearly tuned to higher temporal frequencies than those of females.

mediated by EMDs of the correlation type (see reviews Buchner, 1984; Hausen & Egelhaaf, 1989). Behavioural data provide a remarkable fit to the predictions of the correlation model (Buchner, 1984). Furthermore, similarities between neural responses to behavioural responses and other approaches, as diverse as studying the behaviour of *Drosophila* mutants and lesion studies of tethered flies, provide clear evidence that this behavioural “yaw” response to wide-field motion is driven by inputs from one key class of direction-selective ipsilateral neuron, the so called “HS” cells of the lobula plate (see review by Hausen & Egelhaaf, 1989). Given that the neurons we record from here are, as far as we can tell, analogues (and possibly even homologues) of these HS cells, it seems reasonable to speculate that they play a key role in the ability of these insects to hover.

Recent work on the behavioural responses of the hummingbird hawkmoth, *Macroglossum*, shows that visual cues play an important role in controlling its precise hovering flight (Farina *et al.*, 1994; Farina *et al.*, 1995). This work further demonstrates that the translatory component of optic flow in both frontal and lateral parts of the visual field is compensated for by a velocity-driven (as opposed to a position-driven servo) mechanism mediated by EMDs of the correlation type (Farina *et al.*, 1994; Farina *et al.*, 1995). The properties of the neurons we describe are consistent with a role in such compensation. Interestingly, Wicklein (1994) recently described motion-sensitive neurons (termed “HV” cells) from this species, which respond best to looming or receding stimuli in an opponent manner. Such neurons may be specialised for aiding distance stabilisation (Farina *et al.*, 1994) while feeding from flowers. By analogy to fly HS neurons, those that we describe may be better suited to a role in stabilisation of rotational components of optic flow.

Mechanisms for detecting low and high velocities

Our studies reveal three distinct mechanisms by which neurons of hovering species achieve sensitivity to low velocities: high sensitivity, high spatial resolution and long delay time constants. The temporal tuning curves for *Bombylius* and *Macroglossum* (Fig. 3) contrast greatly with those derived for neurons of bees and butterflies (Maddess *et al.*, 1991; Ibbotson & Goodman, 1990; Bidwell & Goodman, 1993; O’Carroll *et al.*, 1996), which respond optimally to temporal frequencies in the range 10–20 Hz. Since neither bees or butterflies can be considered to be “aerobatic” insects, the much lower temporal frequency optimum in the specialist hoverers we study here is consistent with the special demands of detecting low-velocity motion.

In the large syrphid *Volucella* (a superb hoverer) the optimum velocity of HS-like neurons is, paradoxically, higher than we describe here for *Macroglossum* or *Bombylius* (O’Carroll *et al.*, 1996). Our finding that HS-like neurons of male *Eristalis* have “faster” temporal frequency tuning than in females is consistent with the notion that the tuning of such neurons in syrphids reflect the conflicting demands of diverse behaviour. Despite the “intermediate” temporal frequency optimum, extremely high contrast sensitivity extending to high spatial frequencies results in sensitivity to low velocities without compromising performance at high velocities. This is of obvious importance to animals such as these which suddenly switch from hovering and engage in territorial pursuits at high speed.

Such high visual performance is only achieved at the expense of very large eyes. The 3–4 mm diameter compound eyes of large syrphids like *Volucella* or *Eristalis* are among the largest found in insects. Many visual tasks other than motion detection at low velocities can be expected to play an important role in determining the optimum eye design for these, or any animal. For example, one possible benefit of precise hovering for a male syrphid is the stabilisation of background texture, so that the motion of a foreground target (e.g. a conspecific) “pops out”. Large eyes may benefit the detection and tracking of such small targets (tasks which might not even involve motion detection) as much as the optomotor response. Nevertheless, since eye size ultimately constrains sensitivity to low velocities, it seems reasonable to suggest that the large eyes aid the precise hovering we see in these flies.

Neurons of the bee-fly, *Bombylius*, represent an interesting alternative “strategy” for detection of low velocities without compromising detection of high velocities—the apparent use of two classes of EMDs with different temporal properties, as implied by the dual temporal optima evident in Fig. 3, Figs 5 and 6. Despite eyes which are quite small (diameter approximately 1.5 mm in both sexes), *Bombylius* thus achieves sensitivity over a large range of image velocities (Fig. 5).

The sphingid moth *Macroglossum* also has quite small eyes, with a diameter (approximately 1.7 mm) less than half that of large syrphid flies, but they are of a “diurnal

superposition" design (Bartsch & Warrant, 1994). Although the spatial performance we describe for this species is not as good as that of large syrphid flies (O'Carroll *et al.*, 1996), the very high sensitivity we note for at least one neuron is consistent with the theoretical predictions of high information capacity for this optical design (Land, 1981). Thus, as in syrphids, high absolute sensitivity may help extend useful responses of motion detectors to high, as well as low velocities.

Analysis of rotational optic flow during high speed flight

Interestingly, generation of compensatory responses to rotational components of optic flow experienced during forward flight might involve the same "zero" set point (assuming that the animal is not making a deliberate turn) as during hovering. However, depending on the fine structure of the surrounding world and the forward speed, the flow experienced by tangential neurons such as HS cells will be at higher velocities during rapid progressive flight than during hovering, due to the addition of the translational component of motion associated with the animals progress through its world, particularly in the lateral regions of the visual field. Rather than detecting a deviation from the (desired) zero velocity during hovering, rotation detection during forward flight will thus involve comparison of the difference of the speeds experienced by the two eyes, which might both be high. Similarly, intentional turns (e.g. during conspecific chase behaviour) would shift the "set-point" required for compensatory responses to the speed induced by the turn.

We have observed *Volucella* and *Eristalis* engaged in territorial pursuits at speeds of several metres per second and passing within a few centimetres of nearby vegetation as they do so. Although the speeds experienced would obviously be high, it will require further, detailed analysis of the behaviour to predict the exact nature of the complex optic flow. Analysis of similar pursuit behaviour in the housefly *Fannia*, suggests that rotational speeds of up to 5000 deg/sec are experienced during such manoeuvres (Land & Collett, 1974). At such high rotational speeds, other sensory structures such as the halteres of flies (Nalbach & Hengstenberg, 1994) might play a crucial role in maintaining a desired course. Nevertheless, if visual feedback is used at all, the motion-detecting neurons involved would need to be able to respond to both very high as well as the very low velocities experienced during hovering. Our work shows that in *Bombylius* and large syrphid flies such as *Volucella* and *Eristalis*, different mechanisms provide neurons with responses which reliably encompass a sufficiently large range of image velocities that they are inherently well suited to the demands of such diverse behaviour.

REFERENCES

- Barlow, H. B. & Levick, W. R. (1965). The mechanism of directionally sensitive units in rabbit's retina. *Journal of Physiology*, *178*, 477–504.
- Bartsch, K. & Warrant, E. J. (1994). The nonspherical superposition eye of *Macroglossum stellatarum* (Lepidoptera, sphingidae). In Elsner, N. & Breer, H. (Eds), *Göttingen neurobiology report 1994*. Stuttgart, New York: Thieme.
- Bidwell, N. J. & Goodman, L. J. (1993). Possible functions of a population of descending neurons in the honeybee's visuo-motor pathway. *Apidologie*, *24*, 333–354.
- Borst, A. & Bahde, S. (1986). What kind of movement detector is triggering the landing response of the housefly. *Biological Cybernetics*, *55*, 59–69.
- Borst, A. & Egelhaaf, M. (1987). Temporal modulation of luminance adapts time constant of fly movement detectors. *Biological Cybernetics*, *56*, 209–215.
- Borst, A. & Egelhaaf, M. (1989). Principles of visual motion detection. *Trends in Neuroscience*, *12*, 297–306.
- Buchner, E. (1984). Behavioural analysis of spatial vision in insects. In Ali, M. A. (Ed.), *Photoreception and vision in invertebrates* (pp. 561–621). New York: Plenum.
- Buschbeck, E. K. & Strausfeld, N. J. (1996). Adaptive innovation and phylogenetic conservation of giant lobula plate neurons. A comparison of closely related dipteran species exhibiting different flight behaviour. In Elsner, N. & Schnitzler, H. (Eds), *Brain and evolution* (p. 79). Stuttgart/New York: Thieme.
- Clifford, C. W. G., Ibbotson, M. R. & Langley, K. (1997). An adaptive Reichardt detector model of motion adaptation in insects and mammals. *Visual Neuroscience*, *14*, 741–749.
- Collett, T. S. & Land, M. F. (1975). Visual control of flight behaviour in the hoverfly, *Syrphia pipiens*. *Journal of Comparative Physiology A*, *99*, 1–66.
- Egelhaaf, M., Borst, A. & Reichardt, W. (1989). Computational structure of a biological motion-detection system as revealed by local detector analysis in the fly's nervous system. *Journal of the Optical Society of America A*, *6*, 1070–1087.
- Ellington, C. P. (1984). The aerodynamics of hovering flight. III. Kinematics. *Philosophical Transactions of the Royal Society of London B*, *305*, 41–78.
- Farina, W. M., Kramer, D. & Varjú, D. (1995). The response of a hovering hawk moth *Macroglossum stellatarum* to translatory pattern motion. *Journal of Comparative Physiology A*, *176*, 551–562.
- Farina, W. M., Varjú, D. & Zhou, Y. (1994). The regulation of distance to dummy flowers during hovering flight in the hawkmoth *Macroglossum stellatarum*. *Journal of Comparative Physiology A*, *174*, 239–247.
- Hardie, R. C. (1985). Functional organization of the fly retina. In Ottoson, D. (Ed.), *Progress in sensory physiology* (Vol. 5, pp. 1–79). Berlin: Springer.
- Hassenstein, B. & Reichardt, W. (1956). Systemtheoretische Analyse der Zeit-, Reihenfolgen- und Vorzeichenbewertung bei der Bewegungsperzeption des Rüsselkäfers *Chlorophanus*. *Zeitschrift für Naturforschung B*, *11*, 513–524.
- Hausen, K. (1984). The lobula complex of the fly: structure, function and significance in visual behaviour. In Ali, M. (Ed.), *Photoreception and vision in invertebrates* (pp. 523–559). New York: Plenum.
- Hausen, K. & Egelhaaf, M. (1989). Neural mechanisms of visual course control in insects. In Stavenga, D. & Hardie, R. C. (Eds), *Facets of vision* (pp. 391–444). Berlin: Springer.
- Howard, J., Dubs, A. & Payne, R. (1984). The dynamics of phototransduction in insects: a comparative study. *Journal of Comparative Physiology A*, *154*, 707–718.
- Ibbotson, M. R. & Goodman, L. J. (1990). Response characteristics of four wide-field motion sensitive descending interneurons in *Apis mellifera*. *Journal of Experimental Biology*, *148*, 255–279.
- Kirschfeld, K. (1972). The visual system of *Musca*: studies on optics, structure and function. In Wehner, R. (Ed.), *Information processing in the visual system of arthropods* (pp. 61–74). Berlin: Springer.
- Kirschfeld, K. (1976). The resolution of lens and compound eyes. In Zettler, F. & Weiler, R. (Eds), *Neural principles in vision* (pp. 354–370). Berlin: Springer.
- Kelly, D. H. (1979). Motion and Vision II. Stabilised spatio-temporal threshold surface. *Journal of the Optical Society of America A*, *69*, 1340–1349.

- Land, M. F. (1981). Optics and vision in invertebrates. In Autrum, H. (Ed.), *Handbook of sensory physiology* (Vol. VII/6B, pp. 471–592). New York: Springer.
- Land, M. F. (1992). Visual tracking and pursuit: humans and insects compared. *Journal of Insect Physiology*, *38*, 939–951.
- Land, M. F. & Collett, T. S. (1974). Chasing behaviour of houseflies (*Fannia canicularis*): a description and analysis. *Journal of Comparative Physiology A*, *89*, 331–357.
- Laughlin, S. B. (1996). Matched filtering by a photoreceptor membrane. *Vision Research*, *36*, 1529–1541.
- Laughlin, S. B. & Weckström, M. (1993). Fast and slow photoreceptors—a comparative study of the functional diversity of coding and conductances in the Diptera. *Journal of Comparative Physiology A*, *172*, 593–609.
- Maddess, T., Dubois, R. A. & Ibbotson, M. R. (1991). Response properties and adaptation of neurons sensitive to image motion in the butterfly *Papilio aegaeus*. *Journal of Experimental Biology*, *161*, 171–199.
- Maddess, T. & Laughlin, S. B. (1985). Adaptation of the motion sensitive neuron H1 is generated locally and governed by contrast frequency. *Proceedings of the Royal Society of London B*, *225*, 251–275.
- Nalbach, G. & Hengstenberg, R. (1994). The halteres of the blowfly *Calliphora*. *Journal of Comparative Physiology A*, *175*, 695–708.
- O'Carroll, D. C., Bidwell, N. J., Laughlin, S. B. & Warrant, E. J. (1996). Insect motion detectors matched to visual ecology. *Nature*, *382*, 63–66.
- Payne, R. & Howard, J. (1981). Response of an insect photoreceptor: a simple log-normal model. *Nature*, *290*, 415–416.
- Pick, B. & Buchner, E. (1979). Visual movement detection under light and dark adaptation in the fly, *Musca domestica*. *Journal of Comparative Physiology A*, *134*, 45–54.
- Reichardt, W. (1957). Autocorrelations—Auswertung als Funktionsprinzip des Zentralnervensystems. *Zeitschrift für Naturforschung B*, *12*, 448–457.
- Reichardt, W. (1961). Autocorrelation, a principle for evaluation of sensory information by the central nervous system. In Rosenblith, W. A. (Ed.), *Principles of sensory communication* (pp. 303–317). New York: Wiley.
- van Santen, J. P. H. & Sperling, G. (1985). Elaborated Reichardt detectors. *Journal of the Optical Society of America A*, *2*, 300–321.
- de Ruyter van Steveninck, R., Zaagman, W. H. & Mastebroek, H. A. K. (1986). Adaptation of transient responses of a movement sensitive neuron in the visual system of the blowfly. *Biological Cybernetics*, *54*, 223–236.
- Weckström, M. & Laughlin, S. B. (1995). Visual ecology and voltage gated ion channels in insect photoreceptors. *Trends in Neuroscience*, *18*, 17–21.
- Wicklein, M. (1994). Neuroanatomie der optischen Ganglien und Elektrophysiologie bewegungssensitiver interneurone in der Lobula Platte des Taubenschwanzes *Macroglossum stellatarum* (Sphingidae, Lepidoptera). Dissertation, University of Tübingen, Germany.
- Wilson, H. R. (1985). A model for direction selectivity in threshold motion perception. *Biological Cybernetics*, *51*, 213–222.
- Wolf-Oberhollenzer, F. & Kirschfeld, K. (1994). Motion sensitivity in the nucleus of the basal optic root of the pigeon. *Journal of Neurophysiology*, *71*, 1559–1573.
- Zeil, J. (1993). Orientation flights of solitary wasps (*Cerceris*, Sphecidae, Hymenoptera) 1. Description of flight. *Journal of Comparative Physiology A*, *172*, 189–205.

Acknowledgements—We are greatly indebted to Michael Pfaff and Almut Kelber from the Lehrstuhl für Biokybernetik, University of Tübingen for donation of *Macroglossum* pupae and much useful information. We thank Eric Warrant, Daniel Osorio and John Anderson for useful discussions during the course of this work and for comments on the manuscript. This work was supported by grants from the BBSRC and EPSRC. N. J. Bidwell and R. A. Harris were supported by the Wellcome Trust.